

Optimization of 2D-BM3D Denoising for Long-range Brillouin Optical Time Domain Analysis

Guijiang Yang,¹ Biwei Wang,² Liang Wang,^{1,*} Zhenzhou Cheng,³ Changyuan Yu,² Calvin Chun-Kit Chan,⁴ Litong Li,⁵ Ming Tang,¹ and Deming Liu¹

¹ National Engineering Laboratory for Next Generation Internet Access System, School of Optics and Electronic Information & Wuhan National Lab for Optoelectronics (WNLO), Huazhong University of Science and Technology, Wuhan 430074, China

² Department of Electronic and Information Engineering, The Hong Kong Polytechnic University, Kowloon, Hong Kong.

³ School of Precision Instruments and Optoelectronics Engineering, Tianjin University, Tianjin 300072, China

⁴ Department of Information Engineering, The Chinese University of Hong Kong, Hong Kong

⁵ State Key Laboratory of Optical Fiber and Cable Manufacture Technology, Yangtze Optical Fibre and Cable joint stock limited company, Wuhan 430073, China

*E-mail: hustwl@hust.edu.cn

Abstract: Impact of 2D-BM3D parameters on the denoising performance has been fully analyzed for denoising optimization in 100.8km BOTDA. 12.2dB SNR improvement has been achieved without much loss of temperature accuracy and spatial resolution. © 2020 The Author(s)

OCIS codes: (060.2370) Fiber optics sensors; (290.5900) Scattering, Stimulated Brillouin; (190.4370) Nonlinear optics, fibers.

1. Introduction

Brillouin optical time domain analyzer (BOTDA) has been widely used because of its high-precision distributed temperature and strain measurement [1]. However, due to the noise and fiber loss, the signal-to-noise ratio (SNR) of BOTDA sensing signals becomes worse after long distance transmission, resulting in the degradation of sensing performance. To achieve better performance for sensing distance over 100km, some techniques have been proposed, including optical pulse coding [2], distributed Raman and Brillouin amplifications [3], random fiber laser amplification [4], and time-frequency multiplexing schemes [5]. But most of them rely on the hardware improvement, which increase the complexity of the system and also the cost.

On the other hand, image denoising techniques such as wavelet denoising (WD) and non-local means (NLM) [6] have been applied to enhance the sensing performance, which can improve the SNR without adding hardware complexity. Recently we have experimentally demonstrated the use of 2-Dimensional Block-Matching and 3D filtering (2D-BM3D) for denoising in mid-range BOTDA [7], which shows smaller degradation of the measurement accuracy and experimental spatial resolution compared with WD and NLM. In this paper, we fully analyze the impact of 2D-BM3D parameters on the denoising performance, and optimize them for long-range BOTDA sensing. With the optimized BM3D, we have realized 12.2 dB SNR improvement in 100.8 km sensing range without much degradation of the measurement accuracy and experimental spatial resolution.

2. BOTDA experiment setup

We use a conventional BOTDA setup for the demonstration, which is similar to that in Ref. [7]. The fiber under test (FUT) is a 100.8 km long single-mode fiber with its last 196m section placed in an oven at 60 °C. Another 2.3 m loose fiber segment at the location of 100.6 km is also put in the same oven to verify the measured temperature value and spatial resolution. The fiber section between the 196m and 2.3m sections is 11.8 m long which is kept at room temperature together with the rest of the FUT. A 20 ns pump pulse with a peak power of 20dBm is used. The probe power is -3 dBm. The probe signal is detected by a 125 MHz photodetector and collected on an oscilloscope. The sampling rate of 500 MSample/s and averaging times of 2000 are adopted for data collection.

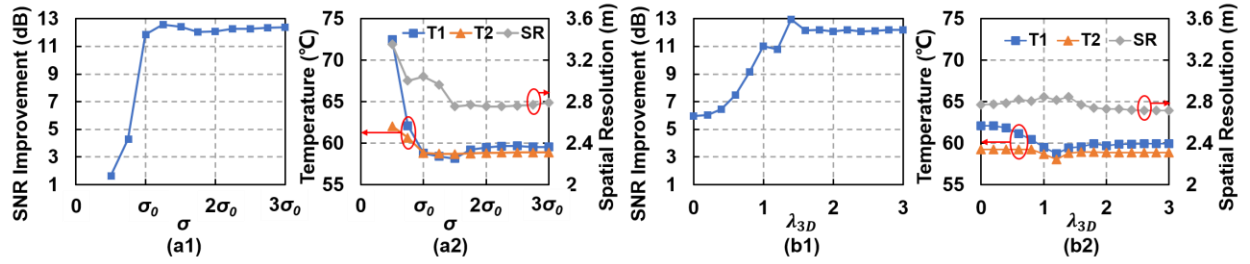
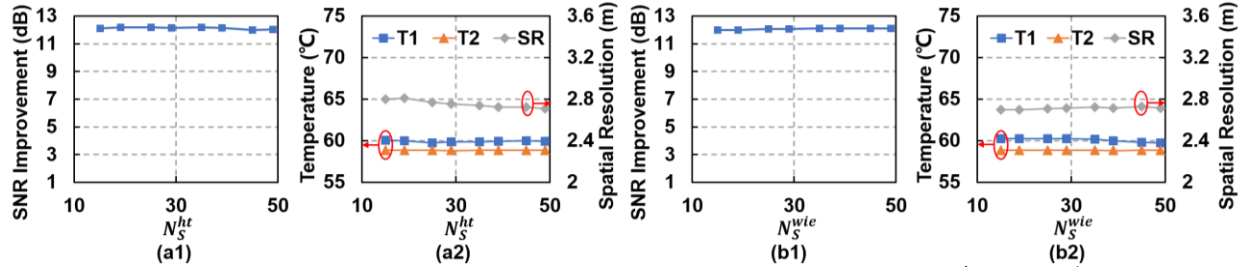
3. Impact of 2D-BM3D parameters on the denoising performance

2D-BM3D denoising is based on the local sparse representation of the image in the transformation domain. By grouping similar 2D image blocks into 3D arrays, it can enhance the data sparsity to effectively denoise them, and at the same time retain most important details of the original image during denoising process [8]. 2D-BM3D has multiple parameters: estimated standard deviation of noise σ , reference block size N_l , maximum number of similar blocks N_2 , distance threshold between two similar blocks τ_{match} , search window size N_s , search-window sliding step N_{step} , threshold for the hard-thresholding λ_{3D} . N_l , N_2 , N_s , N_{step} , and τ_{match} can be further specified as N_l^{ht} and N_l^{wie} , N_2^{ht} and N_2^{wie} , N_s^{ht} and N_s^{wie} , N_{step}^{ht} and N_{step}^{wie} , τ_{match}^{ht} and τ_{match}^{wie} , where *ht* stands for hard-thresholding and *wie* for Wiener filtering. To analyze the impact of the above parameters on the denoising performance, we use the sensing data along the last 300m FUT for demonstration since it has the worst SNR. According to our raw data, we first tentatively set some initial values for those parameters before optimization, as shown in Table. 1.

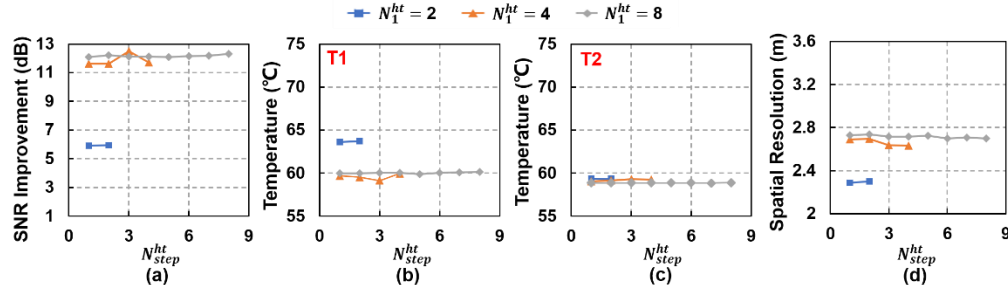
Table 1. Tentative values for the parameters before optimization

N_I^{ht}	N_{step}^{ht}	N_2^{ht}	N_S^{ht}	τ_{match}^{ht}	λ_{3D}	N_I^{wie}	N_{step}^{wie}	N_2^{wie}	N_S^{wie}	τ_{match}^{wie}
8	4	32	39	200	2.5	10	3	32	39	200

Fig. 1 (a) and (b) plot the SNR improvement, measured temperature and spatial resolution as a function of σ and λ_{3D} where T1 & T2 represent the measured temperatures along the 2.3m and 196m heated fiber sections, respectively. Note that $\sigma_0=0.1684$ is the estimated standard deviation of the noise for our raw data. As shown in Fig. 1(a), when σ increases, SNR is improved and better temperature accuracy and spatial resolution have been obtained. There is a little temperature error for the measured temperature along the 2.3m section since there are fewer data points for denoising along the short section [7]. To ensure excellent denoising performance and avoid excessive denoising, the value of σ is finally set to be $2\sigma_0$. Similarly the SNR improvement increases as λ_{3D} increases, as shown in Fig. 1(b1). Small λ_{3D} means weak filtering of the noise in the 3D transform domain, thus excessive residual noise results in poor SNR. When the value of λ_{3D} is larger than 2, the SNR improvement, measured temperature and spatial resolution become stable. So we choose the value of λ_{3D} to be 2.6. The impact of N_S^{ht} and N_S^{wie} on the denoising performance is shown in Fig. 2, where we can see that the value of N_S almost does not affect the denoising performance. But if N_S is large, there is too much irrelevant information during the search process and hence the computational complexity is high. With consideration of this, both the values of N_S^{ht} and N_S^{wie} are selected to be 39.

Fig. 1. SNR improvement, measured temperature and spatial resolution as a function of (a) σ and (b) λ_{3D} .Fig. 2. SNR improvement, measured temperature and spatial resolution as a function of (a) N_S^{ht} and (b) N_S^{wie} .

Then we analyze the impact of both N_I^{ht} and N_{step}^{ht} and the results are shown in Fig. 3. To avoid loss of data details, N_I should be smaller than the number of data points within the spatial resolution (i.e. 10 in our case) [9]. And due to the requirement of data redundancy for denoising N_{step} cannot be larger than N_I . For hard-thresholding, N_I^{ht} must be the power of 2, which means it can take values of 2, 4, 8 in our case. As shown in Fig. 3 (a), when N_I^{ht} is 2, the SNR improvement is small, thus the measured T1 temperature deviates from the real temperature due to small number of data points for denoising. While when N_I^{ht} is increased to 8, the SNR improvement is larger and hence the measured temperatures are close to the real temperature. This is because the redundancy and correlation of

Fig. 3 (a) SNR improvement, (b)&(c) measured temperatures T1 & T2, (d) spatial resolution as a function of N_{step}^{ht} for different values of N_I^{ht} .

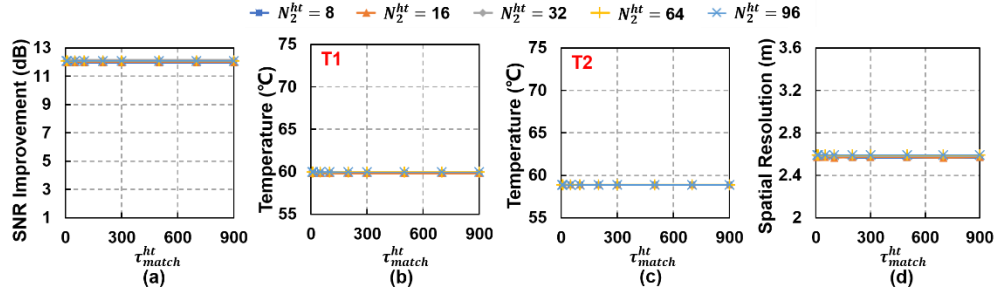


Fig. 4 (a) SNR improvement, (b)&(c) measured temperatures T1 & T2, (d) spatial resolution as a function of τ_{match}^{ht} for different values of N_2^{ht} .

the data increases under large N_I^{ht} . From Fig. 3, we can also find that the impact of N_{step}^{ht} on the denoising is small. Therefore, N_I^{ht} and N_{step}^{ht} are set to be 8 and 6, respectively. In the Wiener filtering, N_I^{wie} and N_{step}^{wie} have similar effects to N_I^{ht} and N_{step}^{ht} , and they are set to be 10 and 5, respectively. At last, we analyze the impact of N_2^{ht} and τ_{match}^{ht} . As shown in Fig. 4, the number of similar blocks and distance between them almost do not affect the denoising performance. Similar results are found for N_2^{wie} and τ_{match}^{wie} . So 32 for N_2 and 200 for τ_{match} are used.

4. Optimized 2D-BM3D denoising for long-range BOTDA sensors

Fig. 5 shows the denoising results using optimized BM3D. Compared with the raw data in Fig. 5(a), the SNR is improved by about 12.2 dB after denoising in Fig. 5(b), and hence the two heated sections are observed clearly, as shown in Fig. 5(c). With denoising, the temperature uncertainty is improved from 8.8 °C to 2.1 °C and the experimental spatial resolution is found to be 2.5m. There is almost no loss of temperature accuracy and spatial resolution when the SNR improvement is maximized.

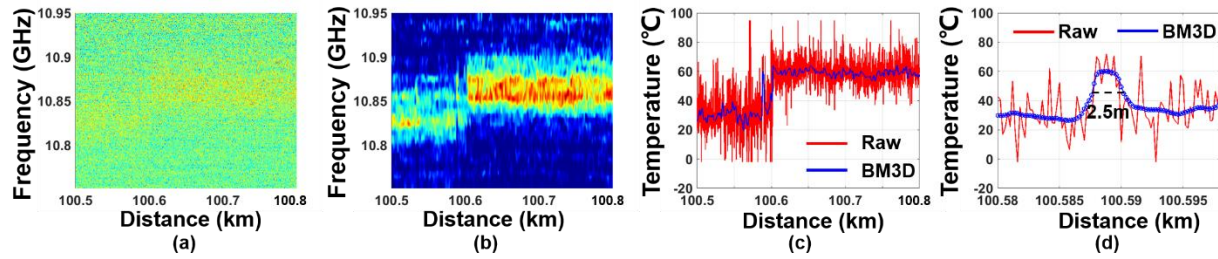


Fig. 5 BGS distribution and temperature distribution along the last 300m FUT before and after denoising.

4. Conclusions

We have designed and optimized 2D-BM3D algorithm for denoising in long-range BOTDA sensor and 12.2dB SNR improvement has been achieved with only small loss of temperature accuracy and spatial resolution. Analysis of the impact of 2D-BM3D parameters on the denoising performance are fully conducted, based on which the parameter optimization has been achieved. We believe the optimized 2D-BM3D denoising would be a powerful tool for ultra-long range BOTDA with less loss of sensing data details.

Acknowledgement

HUST Startup Grant (3004182158, 3011182020), Hubei Provincial Natural Science Foundation of China (2018CFB457), State Key Laboratory of Advanced Optical Communication Systems Networks, China (2020GZKF007).

References

- [1] X. Bao, and L. Chen, *Sensors* 12(7), 8601-8639 (2012).
- [2] M. A. Soto, G. Bolognini, and F. Di Pasquale, *Opt. Lett.* 36(2), 232-234 (2011).
- [3] M. A. Soto et al., *J. Lightwave Technol.* 32(1), 152-162 (2014).
- [4] Yun Fu, R. Zhu, B. Han, H. Wu, Y. Rao, C. Lu, and Z. Wang, *J. Lightwave Technol.* 37(18), 4680-4686 (2019).
- [5] Y. Fu et al., *Sensors* 18(4), 976 (2018).
- [6] M. A. Soto, J. A. Ramírez, and L. Thévenaz, *Nat. Commun.* 7(1), 10870 (2016).
- [7] H. Wu, L. Wang, Z. Zhao, N. Guo, C. Shu, and C. Lu, *Opt. Express* 26(5), 5126-5139 (2018).
- [8] K. Dabov, A. Foi, V. Katkovnik, and K. Egiazarian, *IEEE Trans. Image Process.* 16(8), 2080-2095 (2007).
- [9] M. A. Soto, J. A. Ramírez, and L. Thévenaz, *J. Lightwave Technol.* 36(4), 1168-1177 (2018).